Available online at www.sciencedirect.com
SCIENCE DIRECT®
Journal of Solid State Chemistry 178 (2005) 128–134
JOURNAL OF SOLID STATE CHEMISTRY
www.elsevier.com/locate/jssc

Preparation and characterization of mesoporous TiO_2–CeO_2 nanopowders respond to visible wavelength

Sorapong Pavasupree[a], Yoshikazu Suzuki[a], Sommai Pivsa-Art[b], Susumu Yoshikawa[a,*]

[a]*Institute of Advanced Energy, Kyoto University, Uji, Kyoto 611-0011, Japan*
[b]*Department of Materials and Metallurgical Engineering, Faculty of Engineering, Rajamangala Institute of Technology, Klong 6, Pathumthani 12110, Thailand*

Received 25 August 2004; received in revised form 16 October 2004; accepted 21 October 2004

Abstract

Mesoporous TiO_2–CeO_2 nanopowders responding to visible wavelength were synthesized by using a surfactant assisted sol–gel technique. They were obtained using metal alkoxide precursors modified with acetylacetone (ACA) and laurylamine hydrochloride (LAHC) as surfactant. The samples were characterized by XRD, nitrogen adsorption isotherm, SEM, TEM, and selected area electron diffraction (SAED), respectively. The 95 mol% TiO_2–5 mol% CeO_2 system yielded single anatase phase, however, further addition of the CeO_2 formed cubic CeO_2 structure while anatase TiO_2 decreased. Additions of 5 and 10 mol% CeO_2 increased the surface area, but those of 25, 50, and 75 mol% CeO_2 did not affect it very much. By using this mixed metal oxides system, TiO_2 can be modified to respond to the visible wavelength. The mixed metal oxides had catalytic activity (evaluating the formation rate of I_3^-) about 2–3 times higher than pure CeO_2, while nanosize anatase type TiO_2 materials had no catalytic activity under visible light. The catalytic activity was almost proportional to the specific surface area. The formation rate of I_3^- was much improved by changing the calcination temperature and calcination period. Highest catalytic activity in this study was obtained for the 50 mol% TiO_2–50 mol% CeO_2 nanopowders calcined at 250 °C for 24 h.

Keywords: TiO_2–CeO_2; Mesoporous oxides; Nanopowders; Visible wavelength; Catalytic activity

1. Introduction

Titanium dioxide (TiO_2) and TiO_2-derived materials are of importance for utilizing solar energy. TiO_2 has been widely used for various applications such as a semiconductor in dye-sensitized solar cell, water treatment materials, catalysts and so on [1–5]. Hence many researchers have focused on these materials and attempted to improve their properties. One of the most important properties to improve is catalytic activity of TiO_2. As a first approach, some research groups attempted to modify TiO_2 to respond visible wavelength, e.g., by nitrogen doping [6,7]. Band gap of anatase TiO_2 is about 3.2 eV and thus it can respond only to UV light of wavelength of <400 nm, which is only about 5% of solar energy. If one can modify TiO_2 to respond to visible wavelength of >400 nm (about 45% of solar energy) higher efficiency can be attained. Second approach is to mix with another metal oxide [8,9]. Schattka et al. synthesized porous TiO_2–ZrO_2 mixtures by polymer gel templating and obtained higher catalytic activity than pure component. However, this method resulted in the pore sizes in micro-meter scale [9]. Nanocrystalline particles with controlled size and composition are of technological importance because they have more active sites, enabling to enhance photocatalytic activity [10–14]. In our preliminary works, mesoporous TiO_2 and CeO_2 nanopowders with pore size about 3–6 nm have been synthesized by a modified sol–gel method in an aqueous solution using

*Corresponding author. Fax: +81 774 38 3508.
E-mail addresses: sorapong@iae.kyoto-u.ac.jp (S. Pavasupree), s-yoshi@iae.kyoto-u.ac.jp (S. Yoshikawa).

0022-4596/$ - see front matter © 2004 Elsevier Inc. All rights reserved.
doi:10.1016/j.jssc.2004.10.028

surfactant assisted process, offering rather high photocatalytic activity under UV-light irradiation [15,16]. The mesoporous powder can be also applied for a semiconductor in dye-sensitized solar cells [17,18].

In this study, the surfactant-assisted process has been extended to prepare mesoporous TiO_2–CeO_2 nanopowders respond to visible wavelength. The characteristic of nanopowders and the catalytic activity improvement of the TiO_2–CeO_2 system by changing the composition and calcination conditions will be reported.

2. Experimental

2.1. Synthesis

Mesoporous TiO_2–CeO_2 nanopowders were synthesized using metal alkoxide mixtures modified with acetylacetone (ACA) and laurylamine hydrochloride (LAHC) as surfactant. Tetraisopropylorthotitanate (TIPT, Tokyo Chemical Industry Co., Ltd.) and cerium ^{n}butoxide (Hokko Chemical Industry Co., Ltd.) were used as titanium and cerium sources, respectively. The solution was mixed with acetylacetone (ACA, Nacalai Tesque, Inc), [TIPT + cerium ^{n}butoxide]:ACA = 1:1 in molar ratio, to slowdown the hydrolysis and the condensation reactions. Subsequently, 0.1 M LAHC (Tokyo Chemical Industry Co.) aqueous solution (pH 4–4.5), used as the surfactant solution, was added in the solution (molar ratio of metal alkoixdes mixture to LAHC was 4), and it was stirred at room temperature for 1 h. After kept stirring at 40 °C for 24 h, it was put into an oven at 80 °C for 1 week. The gelation reaction of the solution lead to the release of alcohol as by-product which can be easily removed by drying at 80 °C for 24 h, followed by calcinations at 400 °C for 4 h (Fig. 1). As for some selected TiO_2–CeO_2 compositions, dried samples were washed by 2-propanol and then calcined at 250 °C for 24 h in order to control the mesoporous structure.

2.2. Characterization

The crystalline structure of samples was evaluated by X-ray diffraction (XRD, RIGAKU RINT 2100). The microstructure of the prepared materials was analyzed by scanning electron microscopy (SEM, JEOL JSM-6500FE), transmission electron microscopy (TEM, JEOL JEM-200CX), and selected-area electron diffraction (SAED). The Brunauer–Emmett–Teller (BET) specific surface area was determined by the nitrogen adsorption (BEL Japan, BELSORP-18 Plus). The samples were outgassed overnight at 200 °C before the analyses. Diffuse reflectance spectra were converted from reflection to absorbance by the Kubelka–Munk method [19–21], which measured with a visible spectrophotometer (SHIMADZU, UV-2450) by using $BaSO_4$ as a reference. The catalytic activity was measured through the formation rate of I_3^- due to the oxidation photoreaction of I^- to I_2 in excess I^- conditions [12–14]. 50 mg of sample was added into 10 mL of 0.2 M of potassium iodide aqueous solution then stirred and irradiated with visible light more than 400 nm (Toshiba EFD 12 EN, TSP 100 V, 12 W and UV cut film) with luminance about 10 mW/cm^2. For the formation rate of I_3^- or concentration of I_3^- was determined by using molar extinction coefficient of I_3^- at 288 nm.

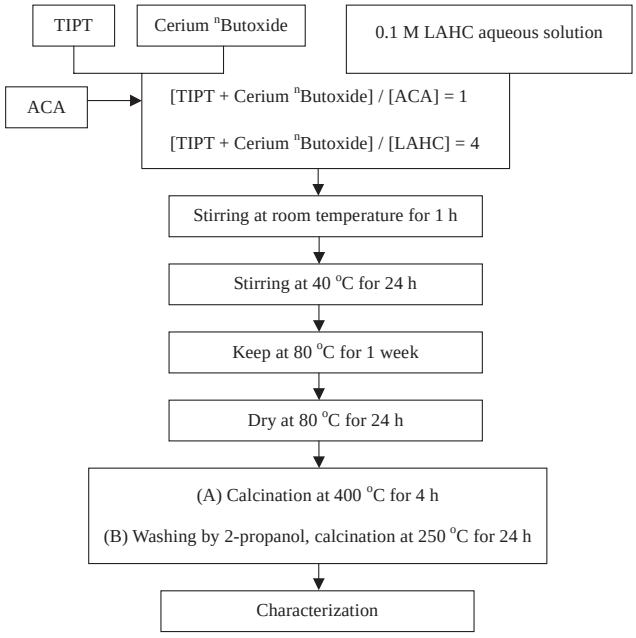

Fig. 1. Schematic representation for experimental procedure.

3. Results and discussion

3.1. CeO_2 addition to TiO_2

Fig. 2 shows the XRD patterns of the prepared TiO_2–CeO_2 nanopowders calcined at 400 °C for 4 h. The 95 mol% TiO_2–5 mol% CeO_2 system yielded single anatase phase, i.e., no cubic CeO_2 was detected. The 75 mol% TiO_2–25 mol% CeO_2 system showed both peak of TiO_2 anatase and cubic CeO_2 but lower crystallinity than each pure component. A further addition of the CeO_2 content (50 and 75 mol% CeO_2) increased cubic fluorite CeO_2 structure while anatase TiO_2 decreased.

Nitrogen adsorption isotherms of these mixed oxides calcined at 400 °C for 4 h showed IUPAC type IV isotherm with sharp inflection of nitrogen adsorbed volume at P/P_0 about 0.65 (type H_2 hysteresis loop), indicating the existence of mesopores (Fig. 3). The pore-size distribution of the sample, as shown in the inset of

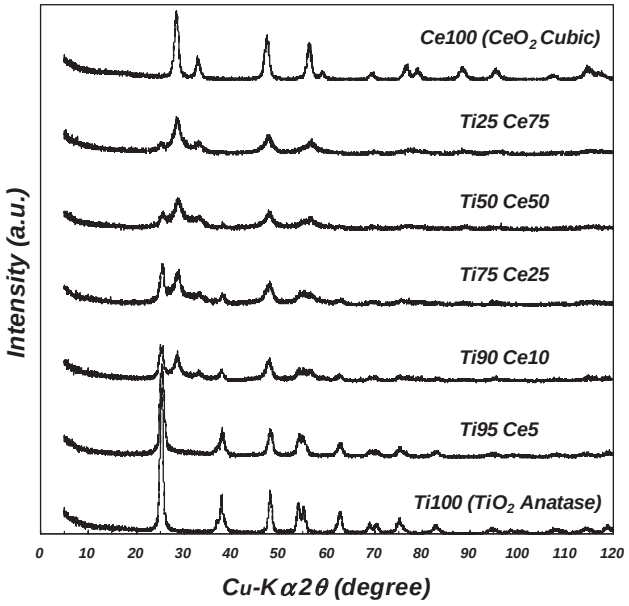

Fig. 2. XRD patterns for the TiO_2–CeO_2 nanopowders calcined at 400 °C for 4 h (molar percent of ceria was varied from 0 to 100).

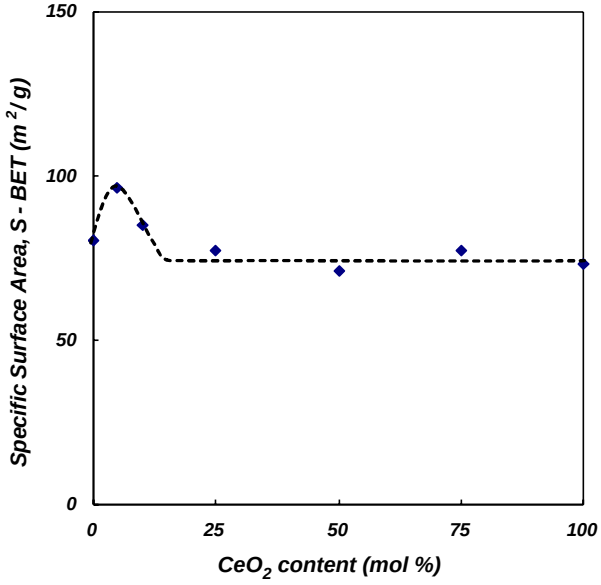

Fig. 4. Specific surface area, for the TiO_2–CeO_2 nanopowders (molar percent of ceria was varied from 0 to 100) calcined at 400 °C for 4 h.

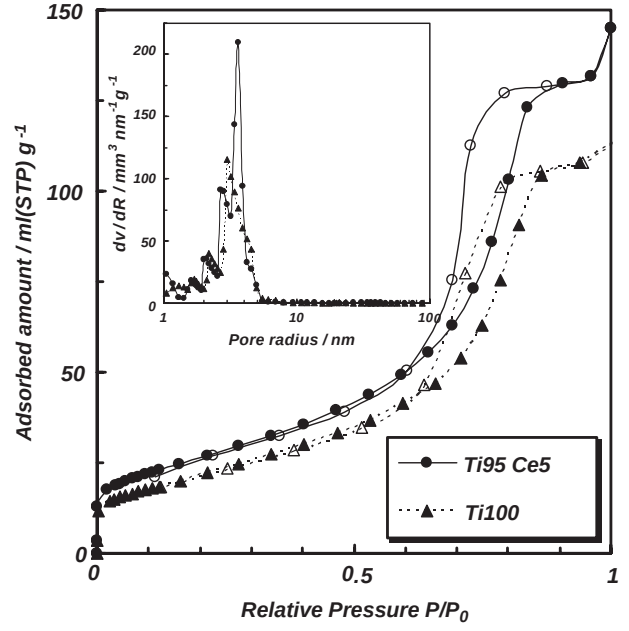

Fig. 3. Nitrogen adsorption isotherm patterns of the 100 mol% TiO_2 (Ti100) and mixed oxides of 95 mol% TiO_2–5 mol% CeO_2 (Ti95 Ce5). The pore size distribution of the samples which have pore size diameter about 5–7 nm (inset).

Fig. 3, showed that the prepared material had mesopores with narrow pore-size distribution (average pore diameter about 5–7 nm).

Fig. 4 gives the BET specific surface area of the TiO_2–CeO_2 system calcined at 400 °C for 4 h. A small addition of CeO_2 to the TiO_2 system by this method increased the specific surface area of the prepared materials. Using a larger amount of CeO_2, the specific surface area decreased, may be due to the CeO_2 segregation, contributing to the reduction of the total surface area [22]. Addition of 25, 50, and 75 mol% CeO_2, did not affect the surface area very much. The BET specific surface area values of the 100 mol% CeO_2 and 100 mol% TiO_2 were 73 and 80 m^2/g, respectively.

TEM images of the TiO_2–CeO_2 nanopowders calcined at 400 °C for 4 h are shown in Fig. 5. Fig. 5(a) shows nanosized crystalline structure of the 100 mol% TiO_2 nanopowder, with the crystalline size about 7–15 nm. The electron diffraction pattern (inset of Fig. 5(a)) supported that the prepared TiO_2 had anatase-type crystalline structure. High-resolution TEM image of the prepared TiO_2 is shown in Fig. 5(b). The lattice fringes of the nanoparticles appearing in the image ($d = 0.35$ nm) also allowed for the identification of the anatase phase.

With 5 mol% CeO_2 addition, nanoparticles became slightly smaller (about 10 nm) and there existed some amorphous like structure of CeO_2 (Figs. 5(c)–(d)). The electron diffraction patterns (inset of Fig. 5(c)) suggested that the crystalline structure of the 95 mol% TiO_2–5 mol% CeO_2 nanopowder was anatase TiO_2, which is agreed with the XRD result. For the 75 mol% TiO_2–25 mol% CeO_2 nanopowder, the crystalline structure of fluorite CeO_2 was observed as shown in Fig. 5(e). The lattice fringes of the nanoparticles appearing in the image demonstrated the crystallographic spacing of the TiO_2 and CeO_2 nanocrystals, most frequently observed for the TiO_2-(101) and CeO_2-(111) crystallographic planes. As the amount of ceria was increased, TiO_2 crystallinity became lower (Figs. 5(g)–(h)), indicating

amorphous-like structure (Figs. 5(i)–(j)). Formation of isolated CeO_2 particles was observed.

TEM image of the 100 mol% CeO_2 (calcined at 400 °C for 4 h) shows nanosize crystallite with the size about 5–10 nm (Fig. 5(k)). The electron diffraction pattern (inset of Fig. 5(k)) supported that the prepared CeO_2 nanopowder had cubic fluorite-type structure. High-resolution TEM image of the CeO_2 nanopowder is shown in Fig. 5(l), indicating the *d*-spacing of 0.31 nm.

In Fig. 6, a representative SEM image of the 50 mol% TiO_2–50 mol% CeO_2 nanopowder is shown. The SEM image indicates that the particles are spherical in nature. Larger particles in this figure should be aggregates of the smaller particles. TiO_2–CeO_2 systems with other composition gave SEM images similar to the mixed oxides of the 50 mol% TiO_2–50 mol% CeO_2 system.

The diffuse reflectance spectra for the TiO_2–CeO_2 nanopowders are shown in Fig. 7. The 100 mol% TiO_2

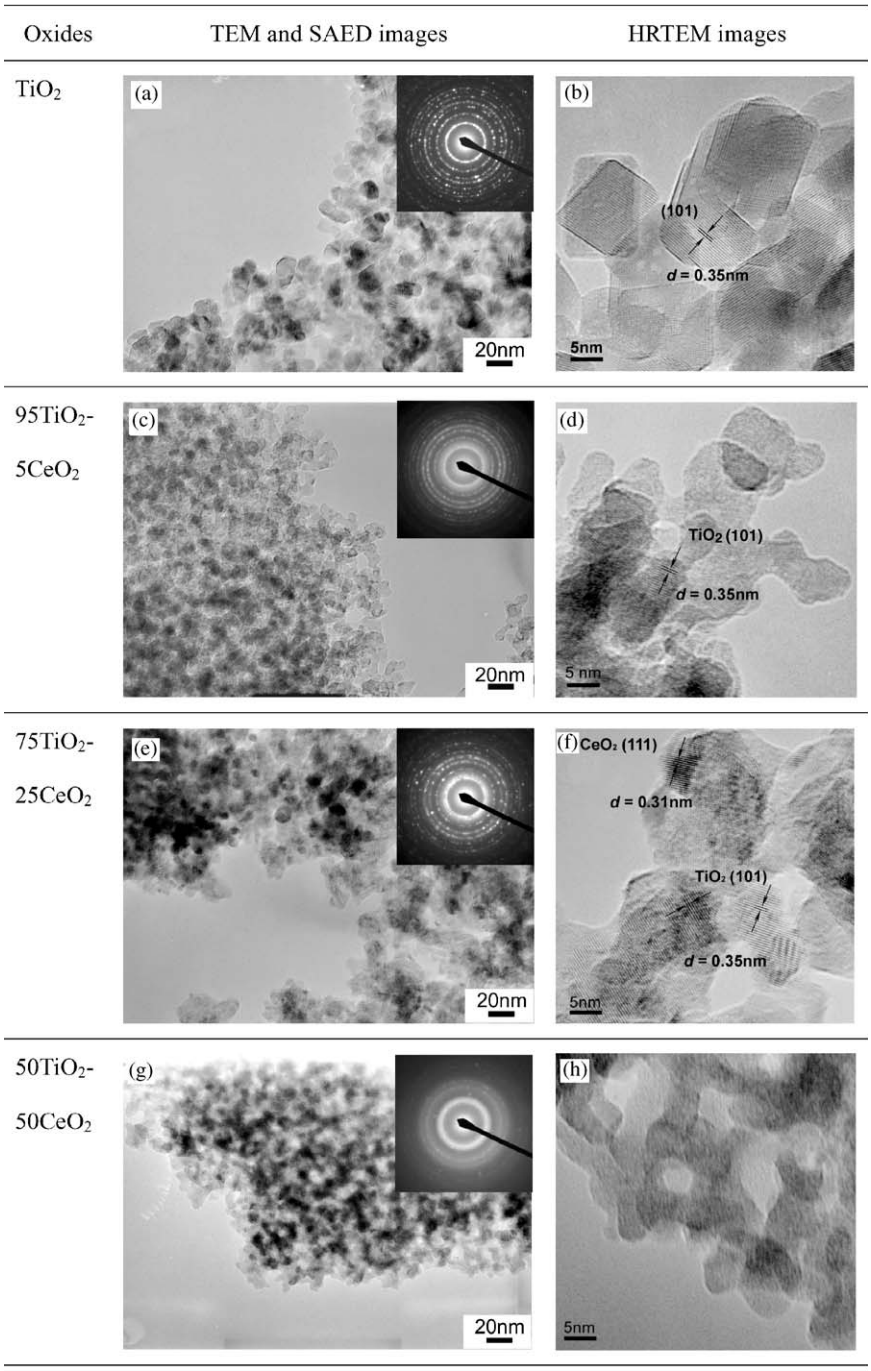

Fig. 5. TEM, SAED, and HRTEM images of the prepared single and mixed metal oxides calcined at 400 °C for 4 h.

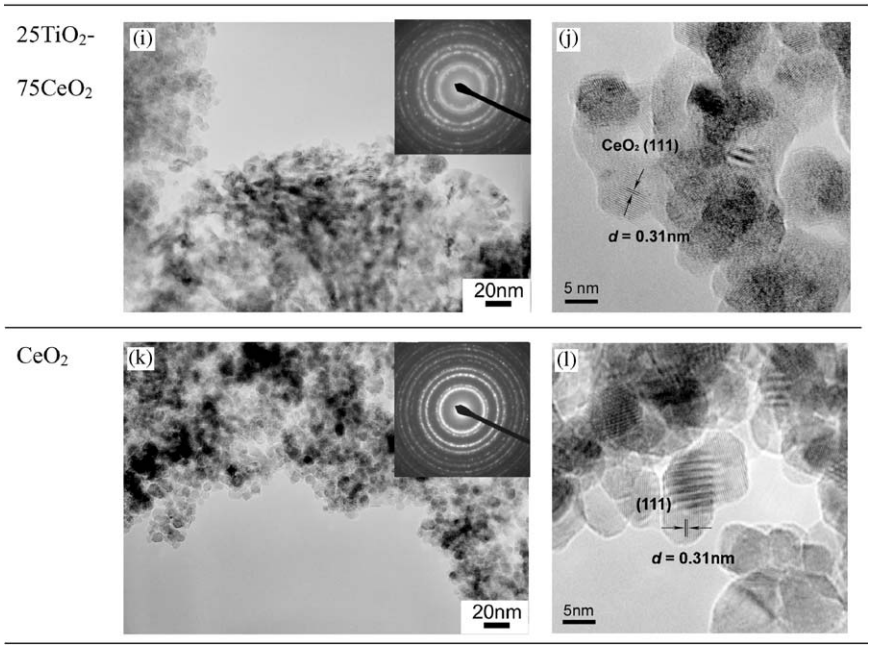

Fig. 5. (*Continued*)

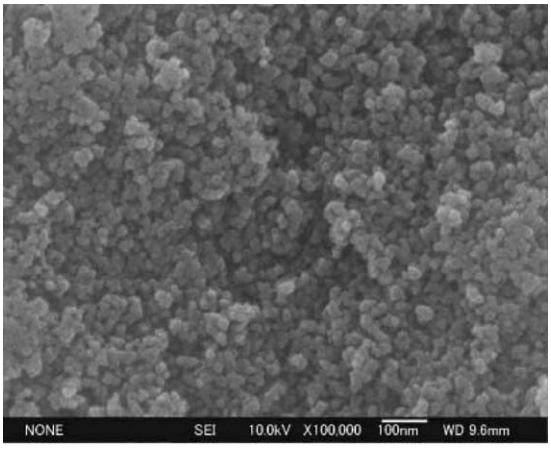

Fig. 6. SEM image of the 50 mol% TiO_2–50 mol% CeO_2 calcined at 400 °C for 4 h.

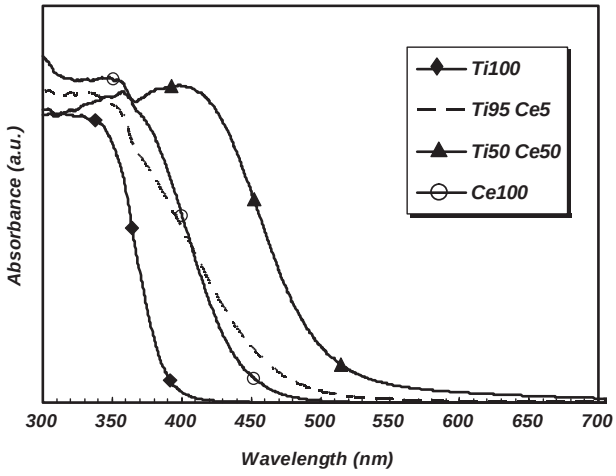

Fig. 7. Diffuse reflectance spectra of the 100 mol% TiO_2 (Ti100), the 95 mol% TiO_2–5 mol% CeO_2 (Ti95 Ce5), the 50 mol% TiO_2–50 mol% CeO_2 (Ti50 Ce50), and the 100 mol% CeO_2 (Ce100).

absorbed light with wavelength shorter than 400 nm (Fig. 7), because the TiO_2 anatase phase has band gap about 3.2 eV. Interestingly, only 5 mol% CeO_2 addition showed red shift of light absorption and can absorb light with the wavelength longer than 400 nm. The best red-shift-light-absorption of mixed oxides was the 50 mol% TiO_2–50 mol% CeO_2 system and it absorbed visible wavelength more than pure component of TiO_2 and CeO_2 [23–24]. The 100 mol% TiO_2 powder was white, the 100 mol% CeO_2 was pale yellow and the mixed oxides of 50 mol% TiO_2–50 mol% CeO_2 was orange-yellow, and therefore the 50 mol% TiO_2–50 mol% CeO_2 system had intensive visible light absorption more than the pure component.

Fig. 8 shows the catalytic activity of the 100 mol% TiO_2 nanopowder, the 100 mol% CeO_2 nanopowder, the 50 mol% TiO_2-50 mol% CeO_2 nanopowder, and a commercial TiO_2 nanopowder (ST01, pure anatase). The 100 mol% TiO_2 and ST01 had no catalytic activity because they cannot absorb visible light (wavelength >400 nm). However, the I_3^- concentration of the 100 mol% CeO_2 was about 0.1×10^{-4} M at 60 min of the irradiation time, indicating that the catalytic activity reaction proceeded. The onset of the action spectrum agreed with that of the absorption spectrum indicating that the catalytic activity proceeded through the band

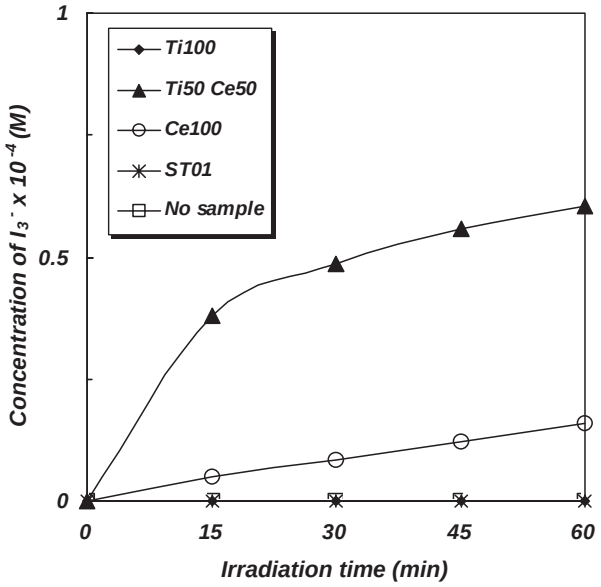

Fig. 8. Catalytic activity of TiO_2 (Ti100), ST01 (commercial anatase type TiO_2), CeO_2 (Ce100), and mixed oxides of 50 mol% TiO_2 with 50 mol% CeO_2 (Ti50 Ce50).

gap excitation. The 50 mol% TiO_2–50 mol% CeO_2 system showed the highest catalytic activity and also higher than about 2–3 times of the 100 mol% CeO_2 because this mixed oxides can absorb visible light at the wavelength longer than the pure component.

3.2. Effect of annealing temperature

Since the 50 mol% TiO_2–50 mol% CeO_2 system showed good catalytic activity, we tried to optimize its microstructure. The particles size of the sample calcined at 250 °C for 24 h was smaller than that calcined at 400 °C for 4 h (Fig. 9). The 50 mol% TiO_2–50 mol% CeO_2 nanopowders calcined at 400 °C for 4 h and 250 °C for 24 h possessed pore-size diameter about 9–10 nm and 4–5 nm, respectively. Their specific surface area were 71 m^2/g and 206 m^2/g, respectively (Table 1). The small pore-size diameter leads to have high surface area.

The I_3^- concentration at 60 min of the irradiation period of the 50 mol%TiO_2–50 mol% CeO_2 calcined at 400 °C for 4 h and 250 °C for 24 h were about 0.6×10^{-4} M and 4×10^{-4} M, respectively (Fig. 10). The high catalytic activity was obtained under the condition of calcination at 250 °C for 24 h. The catalytic activity was much improved by changing the calcination temperature and calcination period because the specific surface area was increased. The catalytic activity depended significantly on calcination conditions. It was almost proportional to the specific surface area. Proportionality between BET surface area and catalytic activity indicates that adsorption of I^- on the materials surface is the rate determining step [12,14].

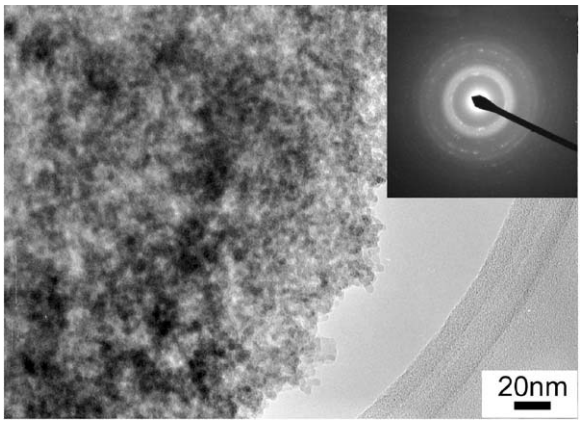

Fig. 9. Representative TEM images of the mixed oxides of 50 mol% TiO_2 with 50 mol% CeO_2 calcined at 250 °C for 24 h, the inset is SAED.

Table 1
Specific surface area of the 50 mol% TiO_2–50 mol% CeO_2 calcined at 400 °C for 4 h and 250 °C for 24 h

Calcination	Specific surface area (m^2/g)
400 °C for 4 h	71
250 °C for 24 h	206

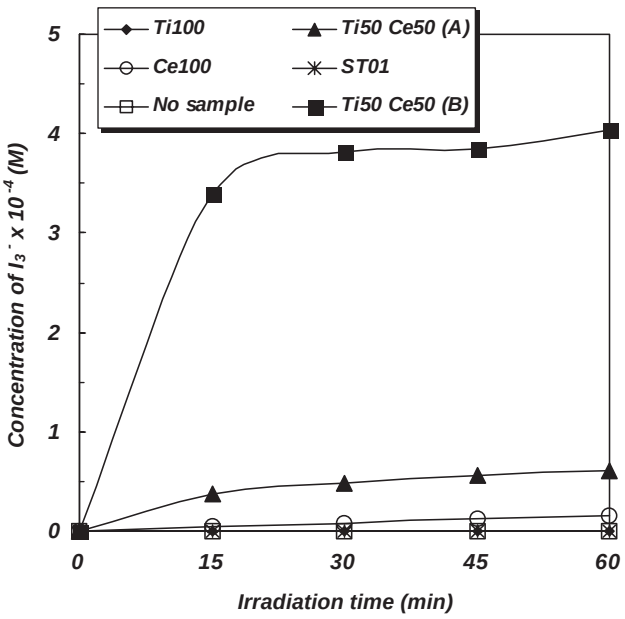

Fig. 10. Catalytic activity of mono oxides, TiO_2, ST01 (commercial anatase type TiO_2), CeO_2 and mixed oxides of 50 mol% TiO_2 with 50 mol% CeO_2 calcined at 400 °C for 4 h (A) and calcined at 250 °C for 24 h (B).

4. Conclusions

The mesoporous TiO_2–CeO_2 nanopowders prepared by the modified sol–gel process (surfactant assisted technique) respond to visible wavelength. A small addition (5 mol%) of CeO_2 did not affect anatase phase. However, further addition of CeO_2 increased fluorite-CeO_2 structure while anatase TiO_2 decreased. Addition of 25, 50, and 75 mol% CeO_2, did not affect the surface area very much. The mixed metal oxides had catalytic activity (I_3^- concentration) about 2–3 times higher than pure CeO_2, while nanosize anatase type TiO_2 materials had no catalytic activity under visible light. This system could control the band gap energy with changing the composition. The formation rate of I_3^- was much improved by changing the calcination temperature and calcination period. The high catalytic activity was obtained under the condition of calcination at 250 °C for 24 h. The synthesis method shown here provides a simple route to fabricate nanostructured materials under mild conditions.

Acknowledgment

The authors would like to express gratitude to Prof. S. Isoda and Prof. H. Kurata, Institute for Chemical Research, Kyoto University for the use of TEM apparatus and Prof. T. Yoko, Institute for Chemical Research, Kyoto University for the use of XRD equipment. Cerium butoxide, zirconium butoxide, and hafnium butoxide were kindly supplied by Hokko Chemical Industry Co., Ltd. This work was supported by a grant-in-aid from the Ministry of Education, Science Sports, and Culture of Japan under the 21 COE program and the Nanotechnology Support Project.

References

[1] B.O. Regan, M. Grätzel, Nature 353 (1991) 737.
[2] M. Grätzel, Nature 414 (2001) 338.
[3] A.L. Linsebigler, G. Lu, J.T. Yates, Chem. Rev. 95 (1995) 735.
[4] A. Fujishima, K. Hashimoto, T. Watanabe, TiO_2 Photocatalysis, Fundamentals and Applications; BKC, Inc., Tokyo, 1999 (Chapter 1).
[5] A. Fujishima, T.N. Rao, D.A. Tryk, J. Photochem. Photobiol. C: Photochem. Rev. 1 (2000) 1.
[6] R. Asahi, T. Morikawa, T. Ohwaki, A. Aoki, Y. Taga, Science 293 (2001) 269.
[7] C. Burda, Y. Lou, X. Chen, A.C.S. Samia, J. Stout, J.L. Gole, Nano Lett. 3 (8) (2003) 1049.
[8] M. Hirano, C. Nakahara, K. Ota, O. Tanaike, M. Inagaki, J. Solid State Chem. 170 (2003) 39.
[9] J. Schattka, D. Shchukin, J. Jia, M. Antonietti, R. Caruso, Chem. Mater. 14 (12) (2002) 5103.
[10] Z. Zhang, C.C. Wang, R. Zakaria, J.Y. Ying, J. Phys. Chem. B 102 (1998) 10871.
[11] H. Zhang, R.L. Penn, R.J. Hamers, J.F. Banfield, J. Phys. Chem. B 103 (1999) 4656.
[12] M. Adachi, Y. Murata, M. Harada, S. Yoshikawa, Chem. Lett. 8 (2000) 942.
[13] M. Adachi, I. Okada, S. Ngamsinlapasathian, Y. Murata, S. Yoshikawa, Electrochemistry 70 (2002) 449.
[14] M. Adachi, Y. Murata, I. Okada, S. Yoshikawa, J. Electrochem. Soc. 150 (8) (2003) G488.
[15] S. Pavasupree, Y. Suzuki, S. Yoshikawa, Proceedings of 14th International Photovoltaic Science and Engineering Conference (PVSEC-14), Bangkok, Thailand, January 26–30, 2004, pp. 185.
[16] S. Pavasupree, Y. Suzuki, S. Pivsa-Art, S. Yoshikawa, Ceram. Int., in press.
[17] S. Ngamsinlapasathian, S. Sakulkhaemaruethai, S. Pavasupree, A. Kitiyanan, T. Sreethawong, Y. Suzuki, S. Yoshikawa, J. Photochem. Photobiol. A 164 (2004) 145.
[18] S. Ngamsinlapasathian, T. Sreethawong, Y. Suzuki, S. Yoshikawa, Sol. Energy Mater. Sol. Cells, 2004, in press.
[19] Y.I. Kim, T.E. Mallouk, J. Phys. Chem. 96 (1992) 2879.
[20] Y.F. Kim, S.J. Atherton, E.S. Brigham, T.E. Mallouk, J. Phys. Chem. 97 (1993) 11802.
[21] A. Kudo, A. Nagane, I. Tsuji, H. Kato, Chem. Lett. (2002) 882.
[22] M.S.P. Francisco, V.R. Mastelaro, P.A.P. Nascente, A.O. Florentino, J. Phys. Chem. B 105 (2001) 10515.
[23] T. Masui, K. Fukuhara, N. Imanaka, T. Sakata, H. Mori, G. Adachi, Chem. Lett. 4 (2002) 474.
[24] K. von Rottkay, T. Richardson, M. Rubin, J. Slack, L. Kullman, Solid State Ion 113–115 (1998) 425.